J Mater Sci: Mater Med (2011) 22:1633–1638
DOI 10.1007/s10856-011-4348-x

Effect of fluorine incorporation on long-term stability of magnesium-containing hydroxyapatite coatings

Yanli Cai · Sam Zhang · Xianting Zeng · Deen Sun

Received: 13 January 2011 / Accepted: 13 May 2011 / Published online: 26 May 2011

Abstract Dissolution resistance and adhesion strength are two main concerns for long-term stability of surface coated metal implants. In this study, fluorine ions are incorporated into magnesium-containing hydroxyapatite coatings (MgF_yHA) via sol–gel method to improve the long-term stability of the implants. Surface and interface are studied in terms of phases, depth profiling and chemical bonds by grazing incidence X-ray diffraction, glow discharge optical emission spectroscopy and X-ray photoelectron spectroscopy. The long-term stability is evaluated by dissolution and pull-off test. The results show that fluorine promotes the incorporation of magnesium in HA lattice. The elemental interdiffusion and chemical bonding take place at the coating/substrate interface. Both the dissolution resistance and the adhesion strength are enhanced by fluorine incorporation, thus the long-term stability of the implant is improved.

1 Introduction

Magnesium (Mg) has its own significance in human body and in bones, thus has been widely incorporated into hydroxyapatite (HA) to develop artificial bone substitutes [1–3]. Yamasaki et al. [4, 5] synthesized functionally graded CO_3 apatite crystals containing Mg ($FGMgCO_3Ap$) as bone substitutes. The results suggested the substitution of Mg ions into apatite crystals might accelerate osteoblast adhesion to apatite and promote bone formation. Biomemetic Mg- and Mg, CO_3-substituted hydroxyapatite were also synthesized by Landi et al. [3]. They found that the doped materials improved the behaviors of MSC and MG63 cells in terms of cell adhesion, proliferation and metabolic activation compared with stoichiometric HA. However, Mg incorporation into HA made the material more soluble in the physiological environment [3, 6]. The enhanced solubility of Mg-substituted HA may, however, affect the long-term stability of bone substitutes. This is especially so when employed as coatings on metal devices, because the high solubility leads the detachment of coating from the substrate before formation of new bone.

The long-term stability study of surface coated medical implants is to relieve mainly two concerns: dissolution resistance of coating and adhesion strength between coating and substrate. In our previous studies [7, 8] as well as in other reported work [9, 10], as fluorine (F) ions were incorporated into HA coatings, stronger dissolution resistance and higher adhesion strength were observed. Fluoridated HA has a more compact crystal structure, better crystallinity and thermal resistance, and reduced coefficient of thermal expansion. Therefore, to counter the dissolution tendency of Mg incorporation, F ions are incorporated into HA simultaneously with Mg for long-term stability.

In this work, Mg and F containing HA coatings are deposited on Ti6Al4V substrate by sol–gel method. The long-term stability is assessed by investigating dissolution resistance and adhesion strength. Also, the phases, the interfacial elements distribution and chemical states, etc.

Y. Cai · S. Zhang (✉)
School of Mechanical and Aerospace Engineering, Nanyang Technological University, 50 Nanyang Avenue, Singapore 639798, Singapore
e-mail: msyzhang@ntu.edu.sg

X. Zeng
Singapore Institute of Manufacturing Technology, 71 Nanyang Drive, Singapore 638075, Singapore

D. Sun
PVD Department Plating Division, Singapore Epson Industrial Pte Ltd, 86 & 88, Second Lok Yang Rd Jurong, Singapore 628162, Singapore

are characterized to elucidate the effect of F ions on the long-term stability of the coatings.

2 Materials and methods

2.1 MgF_yHA coating preparation and characterization

Calcium nitrate tetrahydrate ($Ca(NO_3)_2{\cdot}4H_2O$, Merck, AR) and magnesium nitrate hexhydrate ($Mg(NO_3)_2{\cdot}6H_2O$, Merck, AR) were dissolved in ethanol to prepare 2M of Ca-precursor and Mg-precursor. They were mixed together to form Ca–Mg mixture. 2M of P-precursor was prepared by dissolving phosphorous pentoxide (P_2O_5, Merck, GR) in ethanol followed by a refluxing process for 24 h. Then F-precursor (diluting HPF_6 in ethanol) was added to P-precursor to obtain P–F mixture. The Ca–Mg mixture was added drop-wise into the P–F mixture to form a solution with a (Ca, Mg)/P ratio of 1.67. This mixed solution was further refluxed for 24 h to obtain the sol. The designed fluoridation degree was indicated by y value in the general formula of $Ca_9Mg_1(PO_4)_6F_y(OH)_{(2-y)}$ (MgF_yHA in brief), where y = 0/2, 1/2, 2/2, 3/2 and 4/2, and the corresponding coatings were labeled as MFA0, MFA1, MFA2, MFA3 and MFA4, respectively. Fine polished Ti6Al4V substrate of $20 \times 30 \times 2$ mm^3 was dipped vertically into the sol and withdrawn at a speed of 3 cm/min for the first layer. The as-dipped coating was then dried at 150°C for 15 min followed by firing at 600°C for 15 min. This dipping–drawing–drying–firing process was repeated 4 times at a withdrawal speed of 4.5 cm/min for a thicker coating each time. The final coating thickness was 1.5–2.0 μm. Pure HA ($Ca_{10}(PO_4)_6(OH)_2$) coating was also deposited as control.

Grazing incidence X-ray diffraction (GIXRD, Rigaku Ultima 2000) was employed to analyze the phases of the coatings using CuKα radiation ($\lambda = 0.15406$ nm) at 40 kV and 40 mA with a step size of 0.02. F substitution and concentration in the coatings were measured by X-ray photoelectron spectroscopy (XPS, Kratos-Axis Ultra System) using monochromatic AlKα X-ray source (1486.7 eV). The elements distribution along the depth direction was measured by glow discharge optical emission spectroscopy (GDOES, GD Profiler 2, HORIBA JOBIN YVON). To examine the chemical bonds at the interface of the coating and substrate, the coatings were abraded with SiC sandpapers until the substrate could be seen, then measured by XPS. The measured binding energy was calibrated using C 1s (BE = 284.8 eV).

2.2 Dissolution test

Tris-buffered saline (TBS, 0.9% NaCl, pH 7.4) solution was used to investigate the dissolution behavior of MgF_yHA coatings as well as pure HA coating. Samples were immersed in 25 ml of the TBS solution in sterilized bottles for various periods till 28 days at 37 ± 0.1°C in a water bath. 2 ml of solution was taken out after each period for Ca^{2+} concentrations measurement by an atomic absorption spectroscopy (AAS, SHIMADZU AA-6800). After immersion, the samples were taken out, gently washed using deionized water and dried at room temperature.

2.3 Pull-off test

Adhesion strength of pure HA and MgF_yHA coatings on Ti6Al4V substrate was measured by a universal Instron mechanical testing system (Instron 5569). A clamping fixture was designed to avoid the misalignment during the uniaxial tensile test. Al rod (8-mm-diameter) was glued onto the coating surface with epoxy resin (Epoxy Adhesives DP460, 3M, Scotch-Weld™, USA) and cured at room temperature for 24 h. Then, this rod-sample system was put into the steel holder and the rod was ready for clamping by the Instron fixture as that in our previous studies [11]. In testing, the rod was pulled at a cross-head speed of 1 mm/min until the coating failure. "Pull-off adhesion strength" was used without distinguishing adhesive and cohesive failure, calculated using: $X = 4F/(\pi d^2)$, where X is the "pull-off adhesion strength", F is the actual force applied to the test surface at rupture, and d is the equivalent diameter of the original surface area stressed [12]. Statistical analysis was carried out using one-way analysis of variance (ANOVA) at an average of ten replicates. Differences were considered statistically significant at $p < 0.05$.

3 Results

3.1 Phase and interface analysis

GIXRD profiles of the as-deposited MgF_yHA coatings are shown in Fig. 1. Without F incorporation (MgF_0HA), Mg-substituted β-tricalcium phosphate (β-TCMP) is detected as the main phase, and HA phase exists as the secondary phase. When F is incorporated, FHA becomes the main phase in all the MgF_yHA coatings ($y > 0$).

The elemental distribution from coating to substrate was acquired by GDOES. A typical GDOES depth profile is plotted in Fig. 2, showing the distribution of Ca, P, O, Mg, F, Ti and Al along the depth direction. Three regions are identified at the cross-section along the depth direction: the coating region (R_c), the transitional region (R_t), and the substrate region (R_s). Tangent method is used to determine the boundaries between two adjacent regions. In the coating region R_c, most of the elements in the coating are stable.

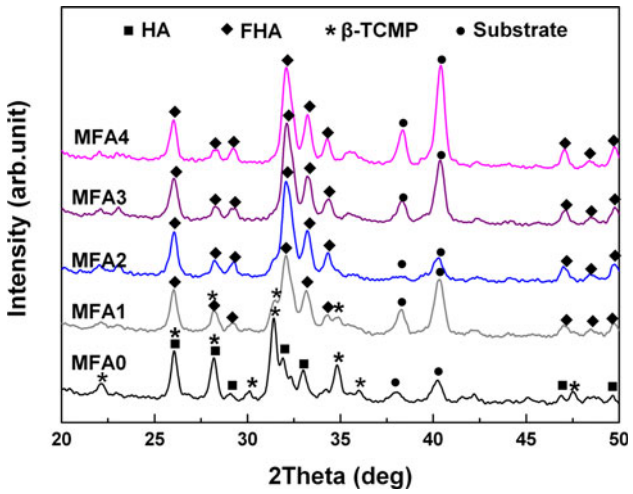

Fig. 1 GIXRD profiles of the as-deposited MgF_yHA coatings on Ti6Al4V substrate

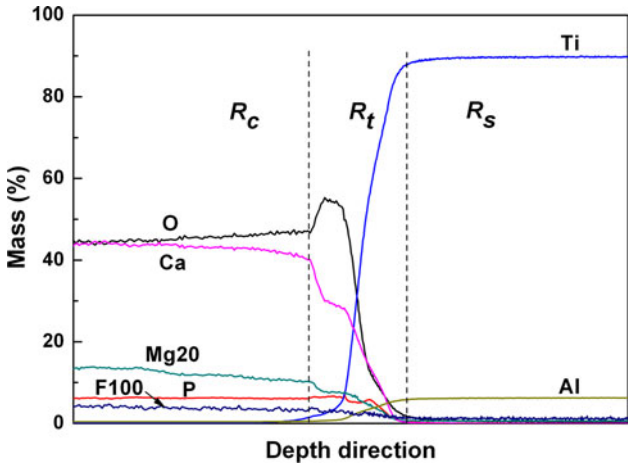

Fig. 2 GDOES depth profile of MFA3 (Mg20: 20 times of Mg concentration; F100: 100 times of F concentration)

At the boundary of R_c and R_t, the concentration of Ca, P, Mg and F begins to decrease, whereas there is an abrupt increase of O concentration followed by a sharp decrease. In the region of R_t, all the elements of the coating as well as the substrate are present. At the boundary between R_t and R_s, Ti and Al stabilize, and Ca, P, O, Mg and F disappear.

XPS narrow scans near the interface of the $MgF_{1.5}HA$ coating and substrate are shown in Fig. 3. The chemical states of Ti, Ca, O and Mg are analyzed. Fig. 3a shows Ti 2p spectrum. Only Ti^{4+} is detected, Ti $2p_{3/2}$ at 458.5 eV and Ti $2p_{1/2}$ at 464.2 eV, the typical binding energy in titanium dioxide (TiO_2) or titanate group (TiO_3^{2-}) [13, 14]. Ca 2p spectrum in Fig. 3b contains 2 different states: Ca $2p_{3/2}$ at 347.4 eV is the typical binding energy of Ca^{2+} in HA or FHA; Ca $2p_{3/2}$ at 346.7 eV can be attributed to $CaTiO_3$ [13, 15]. O 1s spectrum is shown in Fig. 3c. The main component at the binding energy of 529.9 eV can be assigned to O^{2-} species in TiO_2/TiO_3^{2-}, and that at 531.3 eV corresponds to O^{2-} in HA or FHA [13, 15]. P 2p locating at 133.4 eV (not shown here) is attributable to PO_4^{3-} in HA or FHA [15]. Fig. 4d presents Mg 2p spectrum. Only one peak at 50.6 eV is detected, which is the typical binding energy of Mg^{2+}.

3.2 Evaluation of long-term stability

The dissolution resistance of pure HA and MgF_yHA coatings is shown in Fig. 4. All the coatings release more Ca^{2+} ions with the increasing of soaking time. However, pure HA coating releases much more Ca^{2+} ions than all the MgF_yHA coatings during the whole period. Among MgF_yHA coatings, MgF_0HA coating without F incorporation dissolves the fastest, exhibiting the highest Ca^{2+} concentration. When more F ions are incorporated, less Ca^{2+} ions are measured in $MgF_{0.5}HA$, and the least Ca^{2+} concentration in $MgF_{1.0}HA$, $MgF_{1.5}HA$ and $MgF_{2.0}HA$.

As shown in Fig. 5, the pull-off adhesion strength of pure HA coating is only about 10 MPa. When Mg and F ions are incorporated into HA coating, the adhesion strength of MgF_yHA coating is significantly enhanced ($p < 0.05$), but the enhancement of adhesion strength varies when F concentration changes. Without F incorporation (MFA0), the pull-off adhesion strength is about 16 MPa. When F is incorporated at the fluoridation degree of 0.5–1.0, no significant difference is observed compared with MFA0. However, in the range of 1.5–2.0, the pull-off adhesion strength increases significantly compared with MFA0 ($p < 0.05$).

4 Discussion

4.1 Effect of F ions on phase formation

As revealed in Fig. 1, β-TCMP dominates in the MgF_0HA coating. It is due to the presence of Mg ions, because the transformation temperature from apatite to β-TCMP could be lowered about 100°C than that to pure β-TCP (700–800°C) when Mg ions were added. Moreover, the replacement of Ca^{2+} by Mg^{2+} in β-TCP made the structure more stable resulting from the difference in size of Ca^{2+} ions (0.99 Å) and Mg^{2+} ions (0.69 Å) [16]. Since the designed (Ca, Mg)/P ratio in MgF_0HA is 1.67, exceeding the stoichiometric molar ratio of 1.5 for β-TCP, it is understandable that Mg ions preferentially incorporate into β-TCP lattice and the excess of Ca ions form HA phase. When F ions are present, FHA becomes the main phase in all the MgF_yHA coatings ($y > 0$). FHA phase is confirmed by existence of F ions in HA lattice: the main diffraction peaks of HA slightly shift to higher degree [17], and the

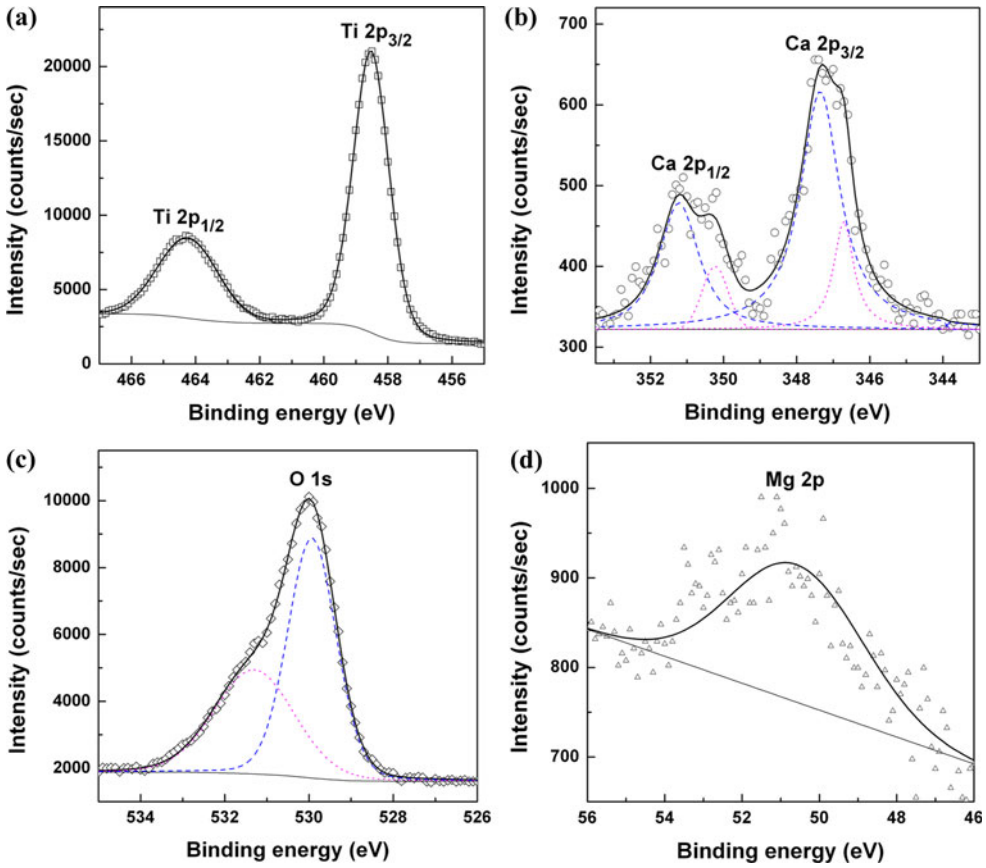

Fig. 3 XPS spectra of Ti 2p a, Ca 2p b, O 1s c and Mg 2p d near the interface of the $MgF_{1.5}HA$ coating and the substrate

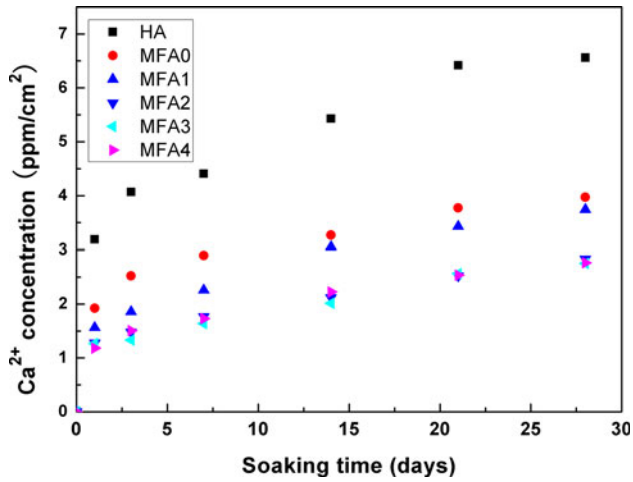

Fig. 4 Dissolution behavior of pure HA and MgF_yHA coatings in TBS solution: Ca^{2+} concentration as a function of soaking time

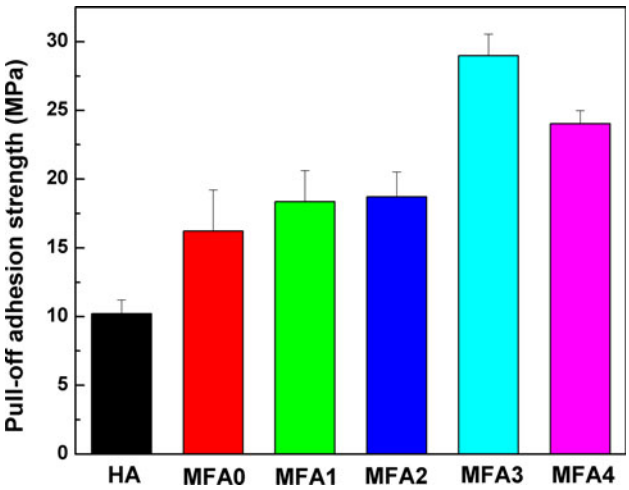

Fig. 5 Pull-off adhesion strength of pure HA and MgF_yHA coatings

typical binding energy of F 1s in FHA locates at 684.3 ± 0.1 eV [8, 18]. Furthermore, it is worthy of noting that when F concentration increases from 0 to 0.5, i.e. $MgF_{0.5}HA$ (MFA1), β-TCMP is only detected with weak intensity; as F concentration further increases, no more β-TCMP forms. This is a clear indication of F ions' suppression ability of β-TCMP formation. In other words, F promotes the substitution of Ca^{2+} with Mg^{2+} in HA lattice, in agreement of our previous findings as well as other researches [6, 19].

4.2 Effect of F ions on long-term stability of Mg-containing HA coating

The dissolution behavior of pure HA and MgF_yHA coatings reveals that the incorporation of Mg and F ions in HA

Table 1 Designed and measured fluorine concentration in MgF_yHA coatings

	$Ca_9Mg_1(PO_4)_6F_y(OH)_{(2-y)}$				
Designed F concentration (y)	0	0.5	1.0	1.5	2.0
Measured F concentration (Y)	0	0.39	0.72	0.97	1.16

coatings greatly improves the dissolution resistance of HA coating. Among MgF_yHA coatings, MgF_0HA coating has the highest dissolution rate, $MgF_{1.0}HA$, $MgF_{1.5}HA$, and $MgF_{2.0}HA$ coating has the lowest but comparable dissolution rate. The dissolution rate is dependent of the solubility of the phases in the coating. From Fig. 1, the phases of MgF_yHA coatings are as follows: most β-TCMP and little HA in MgF_0HA, most FHA and little β-TCMP in $MgF_{0.5}HA$, single FHA in $MgF_{1.0}HA$, $MgF_{1.5}HA$ and $MgF_{2.0}HA$. It is reported that the resorption of calcium phosphates as implants takes place in this order: FHA < Mg-TCP (β-TCMP) < HA < β-TCP < α-TCP [20], because the addition of Mg ions stabilizes the structure of β-TCP [21] and the incorporation of F ions in HA lattice lowers the solubility of HA [7, 10]. Therefore, it is reasonable pure HA coating dissolves the fastest and releases the most Ca^{2+} ions. When Mg and F ions are incorporated into HA coatings, MgF_0HA coating releases the most Ca^{2+} ions, less in $MgF_{0.5}HA$ coating, and the least in $MgF_{1.0}HA$, $MgF_{1.5}HA$ and $MgF_{2.0}HA$ coatings according to the solubility of different phases.

Pull-off test suggests that F incorporation into Mg-containing HA coating enhances the adhesion strength. In pure HA, there is a certain degree of disorder with randomly oriented OH groups. When F ions are incorporated, hydrogen bonds form between OH groups and nearby F ions. Fluorine is very electronegative and has an even greater capacity than oxygen in forming hydrogen bonds. Thus FHA is much more ordered than HA. Theoretically, the structure is the most stable at around 50% substitution due to the alternating arrangement of the F ions between each pair of OH groups [22]. The fluorine concentration measured by XPS is listed in Table 1. There is a discrepancy between the measured and designed F concentration. In $MgF_{1.5}HA$ and $MgF_{2.0}HA$, the measured F concentration is around 1.0 or nearly 50% substitution, thus they have the most stable crystal structure. Correspondingly, significantly higher pull-off adhesion strength is observed in $MgF_{1.5}HA$ and $MgF_{2.0}HA$. Another effect of F ions is the reduction of the coefficient of thermal expansion. The coefficient of thermal expansion of pure HA, pure FA and Ti6Al4V is 15×10^{-6}/K, 9.1×10^{-6}, and 8.9×10^{-6}, respectively. The substitution of F ions in HA lattice reduces the coefficient of thermal expansion, so does the thermal mismatch between the coating and substrate thus the residual stress in the coating is reduced [23]. Furthermore, the chemical bonds such as Ca–O–Ti and Mg–O–Ti bonds revealed in GDOES and XPS at the interface also contribute to the enhancement of the adhesion strength between the coating and substrate.

5 Conclusion

Fluorine promotes the substitution of calcium with magnesium in hydroxyapatite lattice. The elements in the coating and substrate diffuse to each other and form chemical bonds near the coating/substrate interface. Fluorine incorporation into magnesium-containing hydroxyapatite coatings stabilizes the apatite structure and enhances the dissolution resistance as well as the adhesion strength, especially at the measured fluoridation degree around 1.0.

References

1. Bigi A, Foresti E, Gregorini R, Ripamonti A, Roveri N, Shah J. The role of magnesium on the structure of biological apatites. Calcif Tissue Int. 1992;50(5):439–44.
2. Rude RK, Gruber HE. Magnesium deficiency and osteoporosis: animal and human observations. J Nutr Biochem. 2004;15(12):710–6.
3. Landi E, Tampieri A, Mattioli-Belmonte M, Celotti G, Sandri M, Gigante A, et al. Biomimetic Mg- and Mg, CO3-substituted hydroxyapatites: synthesis characterization and in vitro behaviour. J Eur Ceram Soc. 2006;26(13):2593–601.
4. Yamasaki Y, Yoshida Y, Okazaki M, Shimazu A, Kubo T, Akagawa Y, et al. Action of $FGMgCO_3Ap$-collagen composite in promoting bone formation. Biomaterials. 2003;24(27):4913–20.
5. Yamasaki Y, Yoshida Y, Okazaki M, Shimazu A, Uchida T, Kubo Y, et al. Synthesis of functionally graded $MgCO_3$ apatite accelerating osteoblast adhesion. J Biomed Mater Res. 2002;62(1):99–105.
6. LeGeros RZ, Kijowska R, Jia W, LeGeros JP. Fluoride-cation interactions in the formation and stability of apatites. J Fluor Chem. 1988;41(1):53–64.
7. Wang YS, Zhang S, Zeng XT, Ma LL, Weng WJ, Yan WQ, et al. Osteoblastic cell response on fluoridated hydroxyapatite coatings. Acta Biomater. 2007;3(2):191–7.
8. Zhang S, Xianting Z, Yongsheng W, Kui C, Wenjian W. Adhesion strength of sol-gel derived fluoridated hydroxyapatite coatings. Surf Coat Technol. 2006;200(22–23):6350–4.
9. Lee EJ, Lee SH, Kim HW, Kong YM, Kim HE. Fluoridated apatite coatings on titanium obtained by electron-beam deposition. Biomaterials. 2005;26(18):3843–51.
10. Kim HW, Kim HE, Knowles JC. Fluor-hydroxyapatite sol-gel coating on titanium substrate for hard tissue implants. Biomaterials. 2004;25(17):3351–8.
11. Cai Y, Zhang S, Zeng X, Qian M, Sun D, Weng W. Interfacial study of magnesium-containing fluoridated hydroxyapatite coatings. Thin Solid Films. 2011. doi:10.1016/j.tsf.2011.01.007.
12. ASTM. Standard test method for pull-off strength of coatings using portable adhesion testers. ASTM; 2009.02.01 (E2010).
13. Milella E, Cosentino F, Licciulli A, Massaro C. Preparation and characterisation of titania/hydroxyapatite composite coatings obtained by sol-gel process. Biomaterials. 2001;22(11):1425–31.

14. Atuchin VV, Kesler VG, Pervukhina NV, Zhang Z. Ti 2p and O 1s core levels and chemical bonding in titanium-bearing oxides. J of Electron Spectrosc and Relat Phenom. 2006;152(1–2):18–24.
15. Kačiulis S, Mattogno G, Pandolfi L, Cavalli M, Gnappi G, Montenero A. XPS study of apatite-based coatings prepared by sol-gel technique. Appl Surf Sci. 1999;151(1–2):1–5.
16. Kannan S, Ventura JM, Ferreira JMF. Aqueous precipitation method for the formation of Mg-stabilized β-tricalcium phosphate: an X-ray diffraction study. Ceram Intl. 2007;33(4):637–41.
17. Cheng K, Weng W, Wang H, Zhang S. In vitro behavior of osteoblast-like cells on fluoridated hydroxyapatite coatings. Biomaterials. 2005;26(32):6288–95.
18. Cheng K, Zhang S, Weng WJ. The F content in sol-gel derived FHA coatings: an XPS study. Surf Coat Technol. 2005;198(1–3): 237–41.
19. Cai Y, Zhang S, Zeng X, Wang Y, Qian M, Weng W. Improvement of bioactivity with magnesium and fluorine ions incorporated hydroxyapatite coatings via sol-gel deposition on Ti6Al4V alloys. Thin Solid Films. 2009;517(17):5347–51.
20. Tardei C, Grigore F, Pasuk I, Stoleriu S. The study of Mg^{2+}/Ca^{2+} substitution of β-tricalcium phosphate. J Optoelectron Adv Mater. 2006;8(2):568–71.
21. Xue W, Dahlquist K, Banerjee A, Bandyopadhyay A, Bose S. Synthesis and characterization of tricalcium phosphate with Zn and Mg based dopants. J Mater Sci: Mater Med. 2008;19(7):2669–77.
22. Chen Y, Miao X. Thermal and chemical stability of fluorohydroxyapatite ceramics with different fluorine contents. Biomaterials. 2005;26(11):1205–10.
23. Zhang S, Zeng X, Wang Y, Cheng K, Weng W. Adhesion strength of sol-gel derived fluoridated hydroxyapatite coatings. Surf Coat Technol. 2006;200 (22–23 SPEC. ISS.):6350–4.